INTERNATIONAL JOURNAL OF HEAT AND TECHNOLOGY
Vol.33, No.2, 2015
http://dx.doi.org/10.18280/ijht.330201

STUDY OF COMBINED FREE CONVECTION AND SURFACE RADIATION IN CLOSED CAVITIES PARTIALLY HEATED FROM BELOW

S. N. Singh[1] and Dwesh Kumar Singh[2]

[1]Associate professor, Deptt. of Mechanical Engg., ISM Dhanbad, Jharkhand, India, 826004;
[2]Research Scholar, HT Lab, Deptt. of Mechanical Engineering, ISM Dhanbad, Jharkhand, India, 826004.

Email: snsingh631@yahoo.com

ABSTRACT

The results of a numerical investigation of the problem of two-dimensional, steady, incompressible, laminar natural convection with surface radiation from a partially heated bottom wall of closed cavities are reported. The governing equations, written in vorticity-stream function form derived from primitive variable N-S equations, are solved using Finite Volume Method. Results are presented for various parameters in the range of Ra = 10^3-10^6, A = 1-4, W = 0.25-1, ε = 0.05-0.8. For surface radiation calculations, radiosity-irradiation formulation has been used. Based on numerical data, correlations have been developed for convective as well as radiative heat transfers. Results show that Nusselt number increases with the increase of heated bottom part ratio and decreases with the increase of aspect ratio.

Keywords: Closed cavities, Natural convection, Surface radiation, Stream-function, vorticity, Nusselt number, Aspect ratio, partially heated bottom wall.

1. INTRODUCTION

The problem of free and mixed convection heat transfer with surface radiation has gained significant attention in the recent past in the area of thermal control. Despite poor values of heat transfer coefficient, cooling by free convection using air is preferred because of its low cost, inherent reliability, simplicity and noiseless method of thermal control.

To date, many experimental and numerical studies have been conducted on the natural convection heat transfer in the closed cavities. An excellent review of laminar natural convection has been presented by Ostrach [1]. Benchmark numerical solutions for natural convection in a square enclosure with two isothermal and two adiabatic walls have been obtained by de Vahl Davis and Jones [2]. Akiyama and Chong [3] studied the problem for coupled natural convection and radiation in a square enclosure filled with air and having gray surfaces. Using the finite volume method, Mezrhab and Behir [4] studied the heat transfer by radiation and natural convection in an air-filled square enclosure with a vertical partition of finite thickness and varying height. Mahapatra et al. [5] reported a finite element solutionon the interaction of surface radiation and variable property laminar natural convection in a differentially heated square cavity Colomer et al. [6] analyzed the natural convection phenomenon coupled with radiant heat exchange in a three-dimensional differentially heated cavity. Hasnaoui et al [7] have proved numerically the existence of multiple steady-state solutions in the absence of radiation in a rectangular cavity partially heated from below.

Recent back, while studying coupling between radiation and natural convection in a square cavity entirely heated from below, Ridouane et al. [8-9] proved also that the multiplicity of solutions is possible. Recently, Ridouane and Hasnaoui [10] nu+merically studied the effect of surface radiation on multiple natural convection solutions in a square cavity partially heated from below. Singh and Venkateshan [11,13] have presented numerical study of natural convection with surface radiation in partially open cavities. A computational work has been performed in partially partitioned enclosure by Aminossadati and Ghasemi[14]. Effect of radiation on natural convection has been examined by King and Narayanaswamy[15] in multiple partitions enclosure and found that with the increase of number of partitions total Nusselt number reduces even in the presence of surface radiation. M. Nourollahi et al.[16] have proved that Nusselt number is approximately independent of the cavity angle in small Richardson number. K. Lasfer et al.[17] analyzed the laminar natural convection in a side heated trapezoidal cavity at various inclined heated sidewalls. S. Roy et al.[18] have performed a complete heatline analysis on visualization of heat flow and thermal mixing during mixed convection in square cavity with various wall heating. Vivek et al. [19] have presented the interaction effect between natural convection and surface radiation in tilted and shallow cavities.

While much progress has been accomplished in understanding flow and heat transfer in the closed cavities for combined natural convection and surface radiation, there are still some important areas requiring attention. Based on the critical review of the above literature it is clear that the investigation of combined natural convection with surface radiation for partially heated bottom wall have not been examined in detail. So in the present study, heat transfer analysis has been done by placing centrally hot to full bottom hot wall and vertical walls as convective-radiative heat balance adiabatic walls and top horizontal wall as a cold wall of cavities under different geometrical, buoyancy driven and surface radiation conditions.

2. MATHEMATICAL FORMULATION

2.1 Formulation for convection

The two-dimensional, steady, incompressible, laminar natural convection heat transfer from partially central heated bottom wall cavity with height *H*, spacing *d* and heated bottom part ratio W, is considered using the system of coordinates shown in fig. 1. The governing equations in term of stream function (ψ), vorticity (ω), form, for a constant property fluid under the Boussinesq approximation, in the non-dimensional form are:

$$U\frac{\partial \omega}{\partial X}+V\frac{\partial \omega}{\partial Y}=\Pr\left[\frac{\partial^2 \omega}{\partial X^2}+\frac{\partial^2 \omega}{\partial Y^2}\right]-Ra\frac{\partial \theta}{\partial Y} \tag{1}$$

$$\frac{\partial^2 \psi}{\partial X^2}+\frac{\partial^2 \psi}{\partial Y^2}=-\Pr\times\omega \tag{2}$$

$$U\frac{\partial \theta}{\partial X}+V\frac{\partial \theta}{\partial Y}=\frac{\partial^2 \theta}{\partial X^2}+\frac{\partial^2 \theta}{\partial Y^2} \tag{3}$$

$$\text{Where,}\quad U=\frac{\partial \psi}{\partial Y}, V=-\frac{\partial \psi}{\partial X} \text{ and } \omega=\frac{\partial V}{\partial X}-\frac{\partial U}{\partial Y}$$

2.2 Formulation for radiation

The radiosity-irradiation formulation is used to describe surface radiation. The walls are assumed diffuse and gray. For an area element on a boundary of the cavity the non-dimensional radiosity is given by the equation:

$$J_i=\varepsilon_i\left(\frac{T_i}{T_h}\right)^4+(1-\varepsilon_i)\sum_{j=1}^{n}F_{ij}J_j \tag{4}$$

i = 1, 2(m + n - 2)

The view factors $F_{i,j}$ are evaluated using Hottel's crossed string method[11,13].

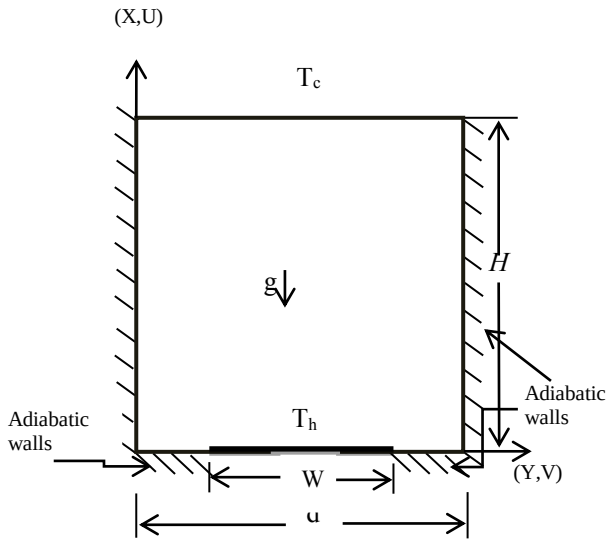

Figure 1.Schematic of the problem geometry

2.3 Boundary conditions

The velocity boundary conditions are based on the assumption that the walls are rigid and impermeable and that the trapped air does not sleep on the walls. In terms of stream function, this assumption can be translated to ψ = 0 at all the surfaces.

At the left and right walls;

$$\psi=0,\ \omega=-\frac{1}{\Pr}\frac{\partial^2 \psi}{\partial Y^2}\ \text{ and }\ \frac{\partial \theta}{\partial Y}=-N_{rc}(J-G)$$

At the top horizontal wall;

$$\psi=0,\ \omega=-\frac{1}{\Pr}\frac{\partial^2 \psi}{\partial X^2}\ \text{ and }\ \theta=0$$

At the adiabatic parts of bottom wall;

$$\psi=0,\ \omega=-\frac{1}{\Pr}\frac{\partial^2 \psi}{\partial X^2}\ \text{ and }\ \frac{\partial \theta}{\partial X}=N_{rc}(J-G)$$

At the centrally heated bottom wall;

$$\psi=0,\ \omega=-\frac{1}{\Pr}\frac{\partial^2 \psi}{\partial X^2}\ \text{ and }\ \theta=1$$

3. METHOD OF SOLUTION

The system of non-dimensional governing equations (1-3) are solved by using well known finite volume method of Gosman et al. [20]. Gauss-Seidel iterative procedure is applied to solve the resulting linear algebraic equations with Successive Under Relaxation (SUR) method. A computer code is developed under FORTRAN platform. As convergence criteria, 10^{-3} is chosen for all dependent variables. Based on grid refinement test, number of grid points are taken as 51 × 51. Results of grid refinement test are presented in the ensuing section. A cosine function have been chosen to generate the non-uniform grids respectively along X and Y directions.

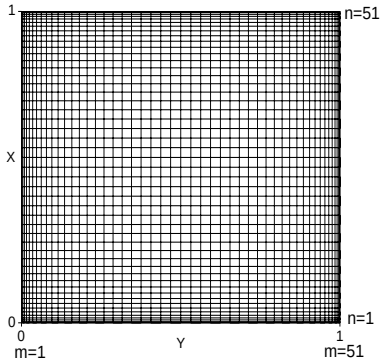

Figure 2. Typical grid pattern

The pattern used is shown in Fig. 2. For derivative boundary conditions, three point formulae using second degree Lagrangian polynomial have been used.

4. RESULTS AND DISCUSSION

Table 1 shows the range of parameters considered in the present study. Calculations have been made keeping in view the objective of evolving useful correlations for the convection and radiation Nusselt numbers.

Table 1. Range of parameters considered in the present study

Parameters	Range
Rayleigh number	1×10^3-1×10^6
Radiation-conduction parameter, Nrc	10.518-56.881
Emissivity, ε	0.05-0.8
Temperature ratio, Tr	0.826-0.901
Aspect ratio	1-4
Heated bottom part ratio, W	0.25-1

4.1 Grid refinement test

Before undertaking a systematic study of the present configurations for the entire range of parameters, the influence of the results on grid is eliminated by conducting a grid refinement check.

Table 2. Grid refinement test

Mesh size	$\overline{Nu}_c$	$\overline{Nu}_r$	$\overline{Nu}_t$	% change in $\overline{Nu}_c$	% change in $\overline{Nu}_r$	% change in $\overline{Nu}_t$
21×21	3.162	9.688	12.85	-	-	-
31×31	3.116	9.768	12.88	1.454	0.819	0.263
41×41	3.105	9.810	12.91	0.353	0.428	0.240
51×51	3.099	9.839	12.93	0.193	0.294	0.177
61×61	3.096	9.848	12.94	0.096	0.091	0.046
71×71	3.095	9.865	12.96	0.032	0.172	0.123
81×81	3.088	9.861	12.95	0.226	0.040	0.077
91×91	3.091	9.871	12.96	0.097	0.101	0.092

This process involved successive refinement of the meshed domain until the difference of two consecutive sets of results agreed to lowest values of the reported heat transfer by convection and radiation from the hot wall. Table 2 shows the effect of the grid size on the solution for a typical case of parameters $Ra=1\times10^5$, A = 1, W = 1, ε = 0.8, N_{rc} = 0.844, T_r = 0.844. The present problem is coupled heat transfer by natural convection and radiation. Since the grid size affects these two to different extents, it is necessary to look at the effect of grid size on both the convection and radiation Nusselt numbers in order to decide the grid system that is to be used to get acceptable results. It can be seen from Table 2 that the difference in $\overline{Nu}_c$, $\overline{Nu}_r$ and $\overline{Nu}_t$ between the grid sizes of 51×51 and 61×61 are 9.6%, 9.1% and 4.6% which are the lowest values. So grid size used in the present problem is fixed to 51×51.

4.2 Code validation

The numerical code is validated by comparing the present results with the benchmark results of Ridouane and Hasnaoui [10], in terms of average convective, radiative Nusselt number and stream function values (ψ_{max}, ψ_{min}) for the case of square cavity partially heated from below to check its validity.

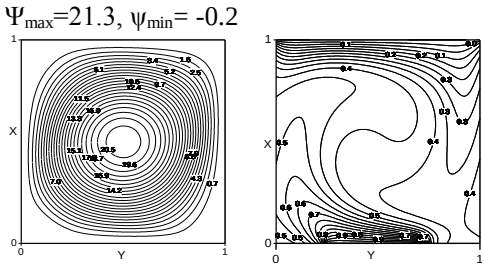

Figure 3. Streamline (left) and isotherm contour (right) for validation

Fig 3 shows the streamline and isotherm contours for parameters $Ra=1\times10^5$, A = 1, W = 0.5, ε = 0.5 of the present study, which are compared with Ridouane and Hasnaoui[10] streamline and isotherm contours for the same above mentioned parameters and are found similar results. For comparison in terms of average Nusselt number, parameters set is taken as $Ra = 6.7\times10^5$, ε = 0.5, A=1, W = 0.5.

Table 3. Comparison of present results

	$Ra=6.7\times10^5$, A=1, W=0.5, ε=0.5			$Ra=1\times10^5$, A=1, W=0.5, ε=0.5	
	$\overline{Nu}_c$	$\overline{Nu}_r$	$\overline{Nu}_t$	Ψ_{max}	Ψ_{min}
Present results	4.38	4.62	9.00	21.30	-0.20
Ridouane results[10]	4.44	4.77	9.22	23.03	-0.19

A comparative result in terms of stream function and Nusselt number are given in Table 3, which clearly shows the good agreement of present result with the bench marked results because of no much deviation in the results.

5. TYPICAL RESULTS FOR CLOSED CAVITIES

Having validated the present code with previous results of Ridouane and Hasnaoui[10], a detailed parametric study has

been undertaken. Typical results from this study are presented here for closed cavities partially heated from below.

5.1 Stream line and isotherm patterns

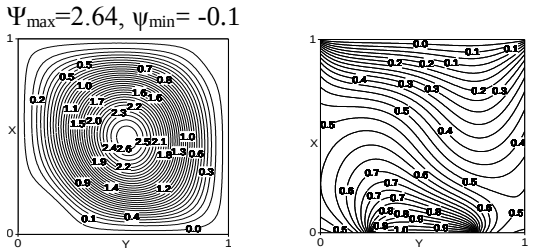

Figure 4. Streamline(left) and isotherm(right) patterns for Ra=7×10^3, A=1, W=0.5, ε=0.5

Figs. 4 and 5 showing the streamline (left) and isotherm (right) contours corresponding to given set of parameters as mentioned against figure captions, indicate the influence of Rayleigh number, Ra. For Ra = 7×10^3, streamline contour of Fig. 4 shows that flow is organized in a multiple loop vortex rotating in clockwise direction.

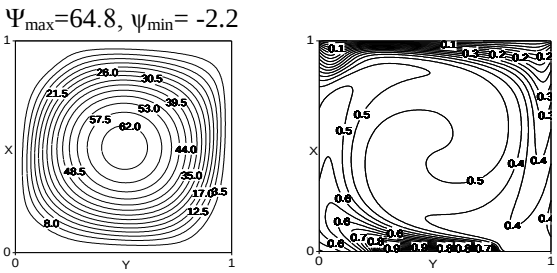

Figure 5. Streamline(left) and isotherm(right) patterns for Ra=1×10^6, A=1, W=0.5, ε=0.5

The corresponding isotherms show weak convection effect and it characterizes a situation for which the conduction regime still dominates. The warm air from the hot element moves up along the left adiabatic wall in vertical direction because of formation of thermal boundary layer due to radiation heat transfer from the bottom heated wall.

At higher value of Rayleigh number, Ra = 1×10^6, Fig. 5 shows the increment of stream function in the core of the cavity, However, the volume flow rate of air(dψ) is smaller with compared to thermal boundary layer region of the walls.. The high curve-linear isotherms obtained at higher Rayleigh number indicate the predominating situation of convection with compared to radiation heat transfer.

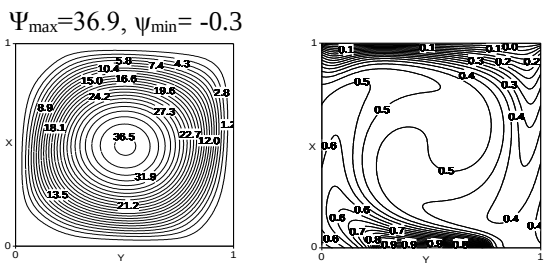

Figure 6. Streamline (left) and isotherm (right) Patterns for Ra=3×10^5, A=1, W=0.5, ε=0.4

Effect of surface radiation for ε = 0.4 and ε = 0.8 on flow and thermal behaviour in the cavities are illustrated in Figs. 6 and 7 for same Rayleigh number, aspect ratio and bottom heating ratio.

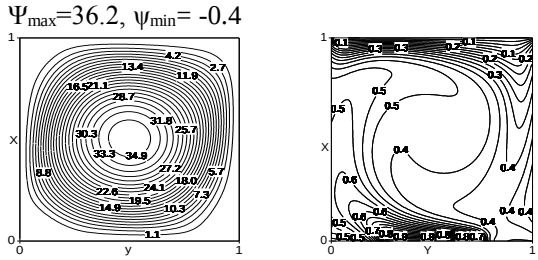

Figure 7. Streamline (left) and isotherm (right) Patterns for Ra=3×10^5, A=1, W=0.5, ε=0.8

By increasing surface emissivity of all the surfaces, the magnitudes of Ψ_{max} and Ψ_{min} are slightly changed as shown in Figs. 6 and 7. The minimum value of stream function shows the existence of secondary vortex in the flow domain. For high value of ε, thermal fields show more steep gradients at the adiabatic walls which increases the strength of thermal boundary layer.

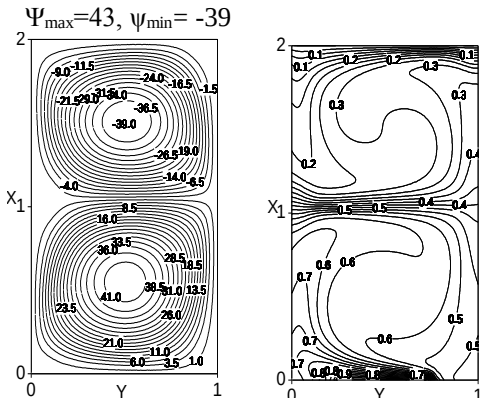

Figure 8. Streamline (left) and isotherm (right) patterns for Ra=5×10^5, A=2, W=0.5, ε=0.1

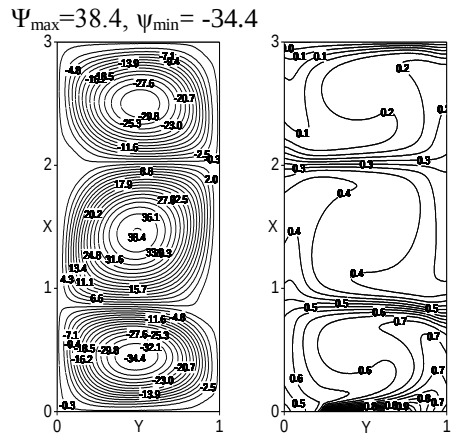

Figure 9. Streamline (left) and isotherm (right) patterns for Ra=5×10^5, A=3, W=0.5, ε=0.1

Streamlines and isotherms in Figs. 8, 9 and 10 for the parameters shown in figures caption are characterized the effect of aspect ratio, A. Figures. 8, 9 and 10 of streamline contours under weak surface radiation condition show the

formation of multi cellular parallel vortices along the vertical wall because of increasing the aspect ratio causing decrement of buoyancy effect. Isotherm patterns in the cavity reveal that the heat is transferred from the heated portion of the bottom wall to the lower part of the next parallel vortex in vertical direction and finally from upper vortex to the cold wall. Fig. 9 for aspect ratio, A=3 show that the three parallel vortices along the height of the cavity are developed, while from Fig. 10 for aspect ratio, A=4 it is found that four parallel vortices are developed along the height of the cavity. So it is observed that as the aspect ratio increases, more stratification loops are obtained. This is due to the fact that the height of the cavity increases in comparison to width, with the increase of aspect ratio, A, which congested the fluid longitudinally and providing more space in vertical direction.

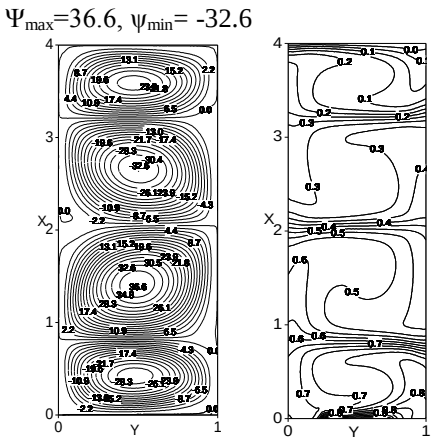

Figure 10. Streamline (left) and isotherm (right) patterns for $Ra=5\times10^5$, A=4, W=0.5, ε=0.1

Therefore air has to travel a longer distance, so tendency of heat transfer by convection reduces, as a result intervening medium, air, of lower vortex transfers heat to the next upper one vortices and finally from top vortex to the cold wall, as it is testified by the presence of sharp gradient of isotherms between the vortices.

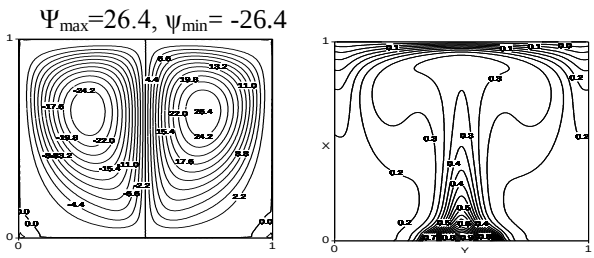

Figure 11. Streamline (left) and isotherm (right) patterns for $Ra=5\times10^5$, A=1, W=0.25, ε=0.1

Figures 11 and 12 presents the influence of aspect ratio on the flow and temperature distribution in the cavity for fixed Rayleigh number, smallest value of bottom part heating ratio and surface emissivity as given against figure captions. Fig. 11 shows that the flow is symmetrical with respect to central heating bottom part of the cavity. In this case bottom heating ratio (W = 0.25) and aspect ratio (A = 1) are smallest and hence formation of a mirror image structure rotates clockwise in the right half and counterclockwise in the left half of the cavity. Both vortices rotate with the same strength ψ = 26.4. The corresponding isotherms shows the heat transfer between the active horizontal walls and the working fluid, mainly in the regions where the hot ascending stream and the cold descending stream enter in contact with these walls. With the increase of aspect ratio A, flow is divided into two vertical parallel vortices along the height of the cavity as illustrated in Fig. 12, lower vortex rotates in the clockwise direction and upper vortex in the counterclockwise direction, which is similar to the case when width of heated portion W= 0.5 and rest of the parameters are same, as mentioned above in Fig. 8. But the strength of lower vortex is reduced with reducing the width of heated portion W, while the strength of upper one is same. Heat flow patterns are same for both cases, when W=0.5 and W=0.25 is considered, as illustrated from Fig. 8 and Fig 12 of isotherm plots.

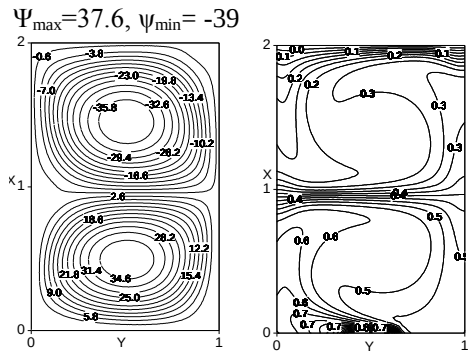

Figure 12. Streamline (left) and isotherm (right) patterns for $Ra=5\times10^5$, A=2, W=0.25, ε=0.1

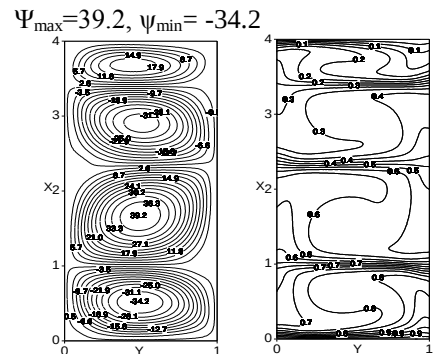

Figure 13. Streamline (left) and isotherm (right) patterns for $Ra=5\times10^5$, A=4, W=1, ε=0.1

Effect of Rayleigh number, Ra for aspect ratio, A=4 and full bottom wall heating, W=1 are illustrated in Figs. 13 and 14 for the parameters shown with the figures caption. Streamline contour of Fig. 13, depicted that four vortices are present in the enclosure along the height of the cavity. As the Rayleigh number, Ra increases five vortices are developed along the height of the cavity, which is presented in Fig. 14, increasing result of vortices loops revealed the condition of more thermal stratification in the cavity. It is because when Rayleigh number, Ra increases, the buoyancy force increases in the vertically upward direction. It causes a strong circulation of fluid inside the cavity, as it can be seen by the increase values of stream function (ψ_{max}, ψ_{min}).This increase in buoyancy force leads to the formation of new vortices loops at top of the cavity. Isotherm patterns in cavity for these two cases show that heat is transferred from bottom

heated wall to the upper cold wall. This is similar to the case of Fig. 10 for the half heated bottom wall, W=0.5.

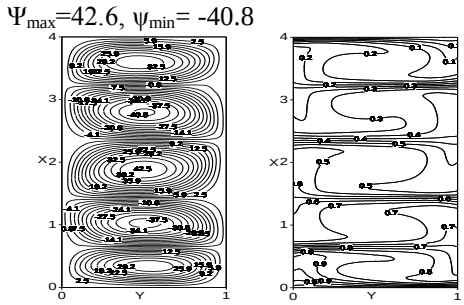

Figure 14. Streamline (left) and isotherm (right) patterns for Ra=1×10^6, A = 4, W=1, ε = 0.1

5.2 Effect of Rayleigh number, aspect ratio, bottom part heating ratio and surface emissivity on Nusselt number

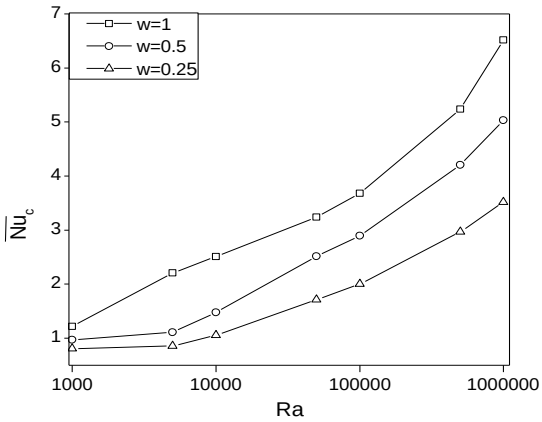

Figure 15. Average convection Nusselt number against Ra for different values of heated portion (W)

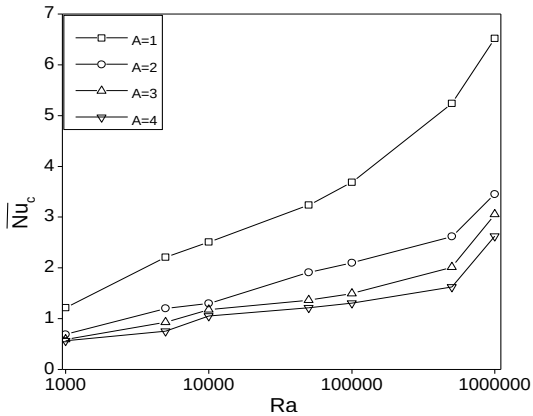

Figure 16. Average convection Nusselt number against Ra for different values of aspect ratio (A)

Figures 15 and 16 show the influence of Rayleigh number, Ra, aspect ratio and bottom heating part on the average convective Nusselt number. Both the Figures show that Nusselt number increases with increase in Rayleigh number causing more cooling effect. As bottom part heating ratio increases the convection effect also increases whereas the Nusselt number decreases with increase in aspect ratio as shown in Fig.16.

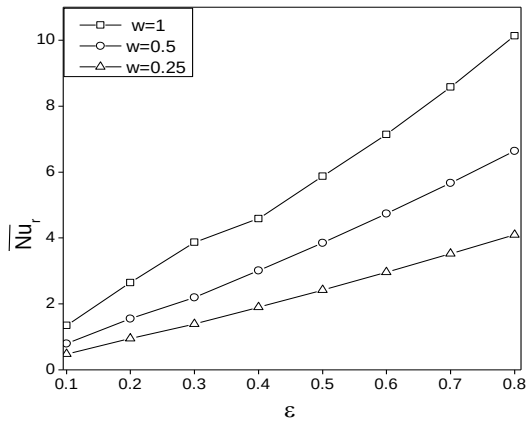

Figure 17. Average radiation Nusselt number against emissivity (ε) for different values of heated portion (W)

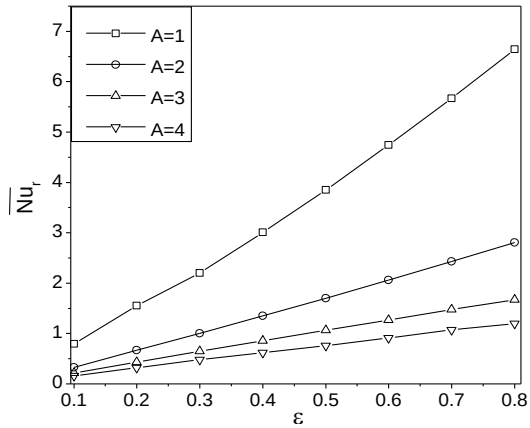

Figure 18. Average radiation Nusselt number against emissivity (ε) for different values of aspect ratio (A)

Figs. 17 and 18 show the influence of surface emissivity, aspect ratio and bottom part heating ratio on radiation Nusselt number for different aspect ratio and W is illustrated in Figs. 17 and 18. Both the above Figures show the increment of radiation Nusselt number with increase in surface emissivity and W whereas the same decreases with increase in aspect ratio which also justifies the earlier statement.

5.3 Variation of total and average Nusselt number with Rayleigh number and emissivity

Fig. 19 is presented for comparison of effect of Rayleigh number, Ra and emissivity, ε on total and average Nusselt number. For a fixed value of Ra, average convection Nusselt number slightly decreases with the increase of ε, which indicates that effect of ε is not more pronounced on the heat transfer by convection, while average radiation Nusselt increases with the increase of ε which illustrates that the radiation heat transfer becomes important for high values of ε. Average convection Nusselt number increases with the increase in Ra whereas average radiation Nusselt number decreases with Ra. Total average Nusselt number increases with the increases of Ra and ε.

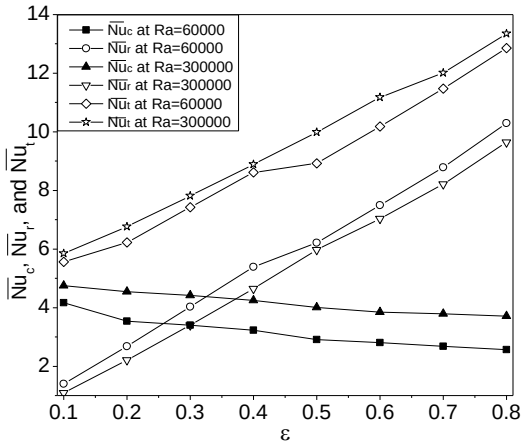

Figure 19. Average convection and radiation Nusselt number against emissivity (ε) for two different value of Ra

6. CORRELATIONS

6.1 Correlation for convection

The range of parameters for which calculation have been done are $10^3 \leq Ra \leq 10^6$, $0.05 \leq \varepsilon \leq 0.8$, $0.826 \leq T_r \leq 0.901$, $10.518 \leq N_{rc} \leq 56.881$, $1 \leq A \leq 4$ and $0.25 \leq W \leq 1$. All the walls were assumed to be of the same emissivity. Based on a large set of data (48 data points), average convection Nusselt number $\overline{Nu}_c$, correlated as

$$\overline{Nu}_c = 0.529 Ra^{0.162} (\varepsilon+1)^{-0.116} (N_{rc}/(N_{rc}+1))^{0.284} A^{-0.210} W^{0.245} \quad (5)$$

As Rayleigh number, Ra directly affects convection heat transfer; its positive exponent shows that heat transfer by convection increases by increasing Ra. N_{rc} is a superflous parameter if only one fluid is considered. But if the temperature level changes, while temperature difference between the heated portion of bottom wall and cold wall remains same, then $\overline{Nu}_c$ will be affected because of radiative effects. Aspect ratio has negative exponent which signifies that heat transfer by convection decreases with the increases of A. In evolving the above correlation, $(1 + \varepsilon)$ term has been used as the most appropriate form for ε, because, even when $\varepsilon = 0$, $\overline{Nu}_c$ would be non-zero, as it still contains convection component and the term has negative exponent , means convection decreases with ε. Width of heated portion, W has positive exponent, which signifies that heat transfer increases with the increase of heated portion of bottom wall. Correlation coefficient of 0.984 and standard error of 0.183 indicates the goodness of fit.

6.2 Correlation for radiation

Average radiation Nusselt number is correlated as

$$\overline{Nu}_r = 1.143 Ra^{-0.009} \varepsilon^{1.021} N_{rc}^{0.820} (1 - T_r)^{0.880} A^{-0.304} W^{0.662} \quad (6)$$

Radiative flux is proportional to $(T_h^4 - T_c^4)$. Hence temperature is correlated in form as given in the equation 6. In regards to T_h, it appears in the N_{rc} term. As ε increases $\overline{Nu}_r$ increases hence the power law form is used for ε. Aspect ratio, A has negative exponent, therefore $\overline{Nu}_r$ decreases with A. Width of heated portion, W follows power law and its exponent is large, therefore $\overline{Nu}_r$ is greatly influenced by W. Influence of convection brought out by the term involving Ra, which shows $\overline{Nu}_r$ decreases with Ra. A very high correlation coefficient of 0.997 and standard error of 0.102 shows the goodness of fit.

7. CONCLUDING REMARKS

It is found that radiation reduces the convective Nusselt number component. Increase of Rayleigh number, Ra enhances the convective heat transfer, while radiation heat transfer decreases up to some extent. For lower value of Ra flow is dominated by conduction, however, as the Ra increases convection takes the role of dominant. Thermal boundary layers develop along all the walls of the cavity. This is a consequence of surface radiation and its interaction with convection. Convective and radiative Nusselt number decreases with aspect ratio, A. Heat transfer increases with the increase of width of the heated portion. Useful correlations for average convective and radiative Nusselt number are presented, encompassing a useful range for various parameters that affect the problem.

REFERENCES

1. S. Ostrach, Natural Convection in Enclosures, *ASME Journal of Heat Transfer*, vol. 110, pp. 1175 –1190, 1988.
2. G. de Vahl Davis and I.P. Jones, Natural Convection in a Square Cavity – A Comparison Exercise, *International Journal of Numerical Methods in Fluids*, vol. 3, pp. 227 – 248, 1983.
3. M. Akiyama and Q.P. Chong, Numerical Analysis of Natural Convection with Surface Radiation in a Square Enclosure, *Numerical Heat Transfer*, Part A, vol. 3 pp. 419 – 433, 1997.
4. A. Mezrhab and A. Behir, Radiation – Natural Convection Interactions in Partitioned Cavities. *Int. J. Numerical Methods Heat Fluid Flow*, vol. 9, pp. 186 – 203, 1999.
5. S. K. Mahapatra, S. Sen and A. Sarkar, Interaction of Surface Radiation and Variable Property Natural Convection in a Differentially Heated Square Cavity – A Finite Element Analysis, *Int. J. Numerical Methods Heat Fluid Flow*, vol. 9, pp. 423– 443. 1999.
6. G. Colomer, M. Costa, R. Consul and A. Oliva, Three Dimensional Numerical Simulation of Convection and Radiation in a Differentially Heated Cavity Using the Discrete Ordinate Method, *Int. J. Heat Mass Transfer*, vol. 47, pp. 257-269, 2004.
7. M. Hasnaoui, E. Bilgen and P. Vasseur, Natural Convection Heat Transfer in Rectangular Cavities Partially Heated from Below, *Journal of Thermo-Physics and Heat Transfer*, vol. 6, pp. 255-264, 1992.
8. E. H. Ridouane, M. Hasnaoui, A. Amahmid and A. Raji, Interaction Between Natural Convection and Radiation in a Square Cavity Heated from Below, *Numerical Heat Transfer-Part A*, vol. 45, pp. 289-311, 2004.
9. E. H. Ridouane, M. Hasnaoui and A. Campo, Effects of Surface Radiation on Natural Convection in a Rayleigh –Benard Square Enclosure Steady and Unsteady Conditions, *Heat and Mass Transfer*, vol. 42, pp. 214-225, 2006.

10. EI. Hassan, E. H Ridouane and M. Hasnaoui, Effect of Surface Radiation on Multiple Natural Convection Solutions in a Square Cavity Partially Heated from Below, *ASME J. Heat Transfer,* vol. 128, pp. 1012-1021, 2006.
11. S. N. Singh and S. P. Venkateshan, Numerical Study of Natural Convection with Surface Radiation Side-Vented Open Cavities, *Int. J. Thermal Sciences,* vol. 43, pp. 865-876, 2004.
12. S. N. Singh and S. P. Venkateshan, Natural convection with surface radiation in partially open cavities, *International Journal of Heat and Technology,* vol. 22, pp. 57-64, 2004.
13. S. N Singh, Numerical study of combined natural convection, conduction and surface radiation heat transfer in open top cavities side vented cavities, *International Journal of Heat and Technology,* vol. 26, pp.101-109, 2008.
14. S. M. Aminossadati and B. Ghasemi, Computational modelling of heat transfer in a partially partitioned enclosure, *International Journal of Heat and Technology,* vol. 26, pp. 61-67, 2008.
15. A. J. C. King and R. Narayanaswamy, Radiative effects on natural convection heat transfer in enclosure with multiple partitions, *International Journal of Heat and Technology,* vol. 27, pp. 1-7, 2009.
16. M. Nourollahi, M. Farhadi, K. Sedighi and A.A.R. Darzi, Numerical investigation of mixed convection in a lid driven cavity at different angles, *International Journal of Heat and Technology,* vol. 27, pp. 87-94, 2009.
17. K. Lasfer, M. Bouzaiane and T. Lili, Numerical study of laminar natural convection in a side heated trapezoidal cavity at various inclined heated sidewalls. *Heat Transfer Engineering,* vol. 31, pp. 362-373, 2010.
18. S. Roy, T. Basak and P.V. Krishna Pradeep, A complete heatline analysis on visualization of heat flow and thermal mixing during mixed convection in square cavity with various wall heating, *Industrial and engineering Chemistry Research,* vol. 50, pp. 7608-7630, 2011.
19. V. Vivek, A.K. Sharma and C. Balaji, Interactions effects between natural convection and surface radiation in tilted square and shallow cavities, *International Journal of Thermal Sciences,* vol. 60, pp. 70-84, 2012.
20. A. D. Gosman, W.M. Runchal Pun, A.K. Spalding and D.B. Wolfshtein, *Heat and Mass Transfer in Rectangular Flows.* Academic Press, London, 1969.

NOMENCLATURE

A aspect ratio, H/d
d spacing……..……..……m
$F_{i,j}$ view factor between element i and j
g acceleration due to gravity…….……m/s^2
G' elemental irradiation……W/m^2
G elemental dimensionless irradiation, $G'/\sigma T_h^4$
H height of the cavity, ……..……m
J' elemental radiosity…..……W/m^2
J elemental dimensionless radiosity, $J'/\sigma T_h^4$
k conductivity of air……..W/m-K
N_{rc} radiation conduction parameter, $\sigma T_h^4 d/[(T_h - T_{cd})k]$
Nu_c local convection Nusselt number , $-\left(\frac{\partial \theta}{\partial X}\right)_{X=0}$
$\overline{Nu}_c$ average convection Nusselt number, $\int_{(1-W)/2}^{(1+W)/2} Nu_c dX$
Nu_r local radiation Nusselt number, $N_{rc}(J-G)$
$\overline{Nu}_r$ average radiation Nusselt number , $\int_{(1-W)/2}^{(1+W)/2} Nu_r dX$
$\overline{Nu}_t$ total Nusselt number, $\overline{Nu_c} + \overline{Nu_r}$
m number of grid points in horizontal direction in the computational domain
n number of grid points in vertical direction in the computational domain
Pr Prandtl number, υ/α
Ra Rayleigh number, $g\beta(T_h - T_c)H^3/(\upsilon\alpha)$
T temperature……K
T_h temperature of partially and full heated bottom wall……..……K
T_c temperature of cold upper wall……K
T_r temperature ratio, T_c/T_h
u vertical velocity…….……..….m/s
U dimensionless vertical velocity, ud/α
v horizontal velocity…….……...m/s
V dimensionless horizontal velocity, vd/α
w centrally heated bottom part……..……m
W heated bottom part ratio wall, w/d
x vertical coordinate…….....……m
X dimensionless vertical coordinate, x/d
y horizontal coordinate…….……m
Y dimensionless horizontal coordinate, y/d

Greek symbols

α fluid thermal diffusivity…….……m^2/s
β isobaric coefficient of volumetric thermal expansion, 1/T……..……..…..1/K
ε emissivity of the walls
υ kinematic viscosity of the fluid ……..….m^2/s
θ dimensionless temperature, $(T - T_c)/(T_h - T_c)$
Ψ' stream function…….……..……m^2/s
Ψ dimensionless stream function, ψ'/α
ω' vorticity……...1/s
ω dimensionless vorticity, $\omega' d^2/\upsilon$
σ Stefan Boltzmann constant, 5.67×10^{-8} W/m^{2}k^4

Subscripts

h hot
c convection, cold
i,j any two arbitrary area element
r radiation, ratio
rc radiation-conduction

Superscript

, dimensional term